



# HHS Public Access

Author manuscript

Cell Rep. Author manuscript; available in PMC 2018 August 15.

Published in final edited form as:

Cell Rep. 2018 June 12; 23(11): 3152–3159. doi:10.1016/j.celrep.2018.05.053.

## Progressive Upregulation of Oxidative Metabolism Facilitates Plasmablast Differentiation to a T-Independent Antigen

Madeline J. Price<sup>1</sup>, Dillon G. Patterson<sup>1</sup>, Christopher D. Scharer<sup>1</sup>, and Jeremy M. Boss<sup>1,2,\*</sup>

<sup>1</sup>Department of Microbiology and Immunology and the Emory Vaccine Center, Emory University School of Medicine, Atlanta, GA 30322, USA

### SUMMARY

Transitioning from a metabolically quiescent naive B cell to an antibody-secreting plasmablast requires division-dependent cellular differentiation. Though cell division demands significant ATP and metabolites, the metabolic processes used for ATP synthesis during plasmablast formation are not well described. Here, the metabolic requirements for plasmablast formation were determined. Following T-independent stimulation with lipopolysaccharide, B cells increased expression of the oxidative phosphorylation machinery in a stepwise manner. Such activated B cells have increased capacity to perform oxidative phosphorylation but showed dependency on glycolysis. Plasmablasts displayed higher oxidative metabolism to support antibody secretion, as inhibiting oxidative ATP production resulted in decreased antibody titers. Differentiation by Blimp1 was required for this increase in oxidative metabolism, as Blimp1-deficient cells proliferate but do not upregulate oxidative phosphorylation. Together, these findings identify a shift in metabolic pathways as B cells differentiate, as well as the requirement for increased metabolic potential to support antibody production.

### Graphical abstract

**In Brief** Price et al. identify a metabolic switch in B cells that is required for maximal antibody secretion. Proliferating, activated B cells switch from glycolysis to oxidative phosphorylation as they differentiate into plasmablasts.

---

This is an open access article under the CC BY-NC-ND license (<http://creativecommons.org/licenses/by-nc-nd/4.0/>).

\*Correspondence: jmboss@emory.edu.

<sup>2</sup>Lead Contact

### SUPPLEMENTAL INFORMATION

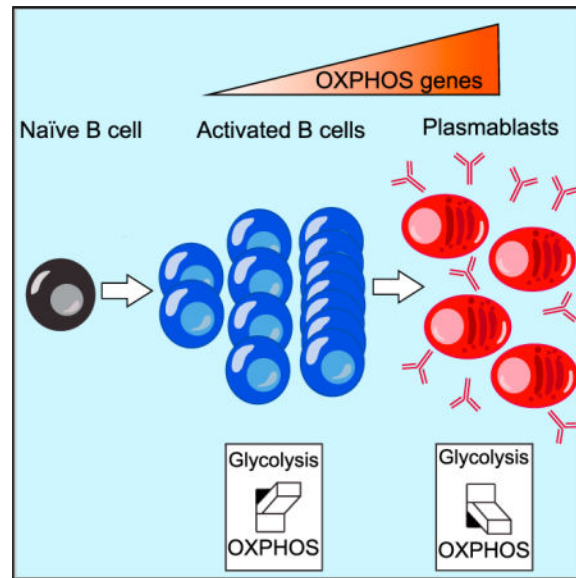
Supplemental Information includes Supplemental Experimental Procedures and can be found with this article online at <https://doi.org/10.1016/j.celrep.2018.05.053>.

### AUTHOR CONTRIBUTIONS

M.J.P. designed and performed experiments, analyzed data and wrote the manuscript. D.G.P. performed experiments. C.D.S. performed bioinformatic analyses. J.M.B. designed experiments and wrote the manuscript. All authors edited the manuscript.

### DECLARATION OF INTERESTS

The authors declare no competing interests.



## INTRODUCTION

Humoral immunity is characterized by the presence of antibody-secreting plasmablasts (PBs), which are derived from the proliferation and differentiation of B cells. B cells undergo significant morphologic and bioenergetic changes to support their transition from quiescent naïve B (nB) cells to PBs, including upregulation of metabolism to support the initial proliferative demands of activated B (actB) cells and, ultimately, the translational demands of PBs (Aronov and Tirosh, 2016; Dufort et al., 2007). For example, following B cell receptor stimulation, actB cells upregulate the expression of Glut1, a cell-surface glucose transporter. Glycolysis and oxidative phosphorylation (OXPHOS) are both increased upon B cell receptor and Toll-like receptor (TLR) stimulation (Caro-Maldonado et al., 2014; Doughty et al., 2006; Woodland et al., 2008). The kinetics of metabolic upregulation that nB cells undergo during the process of differentiation to PB have not been characterized.

Studies in T cell metabolism identified metabolic changes that facilitate differentiation to effector or memory cells (Chang et al., 2013; Fox et al., 2005). In long-lived plasma cells, metabolic differences, including the import of pyruvate into the mitochondria, occur and are believed to aid in their long-term survival (Lam et al., 2016). Though metabolic demands change as immune cells become activated and acquire distinct functions, the metabolic changes associated with cell division versus differentiation remain to be defined.

Here, we report a progressive increase in the expression of genes associated with primary metabolic functions during the initial proliferative stage as B cells differentiate. We find that increased metabolic demand is driven, first, by cellular division and, later, by differentiation. Furthermore, we find that expression of the master regulator of PB differentiation, Blimp1, was required for maximal metabolic activity. These data, therefore, link the B cell transcriptional and differentiation programs to increased metabolic capacity of PB, allowing these cells to execute their function.

## RESULTS

### Metabolism Changes Correspond with Differentiation State

To determine whether metabolic pathways were regulated at the level of gene expression, previously collected gene expression data (Barwick et al., 2016) during B cell differentiation was reanalyzed. In those experiments, cell-trace-violet (CTV)-labeled nB cells were transferred to B cell-deficient mMT mice and challenged with TLR4 agonist, lipopolysaccharide (LPS). After 3 days, the transferred splenic cells were sorted based on their cell division status, and the transcriptomes of cells representing the early (divisions 0, 1, and 3), middle (divisions 5 and 8) and late (division 8+) stages of differentiation were determined. Divisions 8 and 8+ signify the CD138 status (-/+) of cells that have undergone at least 8 divisions. Division 8+ cells have the characteristics of PBs (Barwick et al., 2016; Smith et al., 1996). This analysis showed a stepwise upregulation of genes involved in both the tricarboxylic acid (TCA) cycle (Figures 1A and 1B) and the electron transport chain (ETC) (Figure 1C), the two components of OXPHOS. Six TCA genes were upregulated as the cells progressed through their divisions to PBs, including *Sdhb*, *Sdhb*, *Sdhd*, *Sdha*, *Sdhc*, and *Pdhb*. The most upregulated TCA gene, *Sdhb*, encodes succinate dehydrogenase subunit B, which oxidizes succinate to fumarate. The succinate dehydrogenase complex also participates in the ETC by reducing ubiquinone (Guzy et al., 2008), thereby bridging the TCA cycle and the ETC.

At least 30 ETC genes were also upregulated as B cells progressed to PBs, including *Atp5g2*, *Atp5h*, *Atp5e*, *Atp5o*, and *Uqcrl10* (Figure 1C). The most upregulated gene, *Atp5g2*, encodes a subunit of the mitochondrial ATP synthase complex (complex V), which catalyzes ADP to ATP using the proton gradient established by ETC complexes I–IV. Importantly, inhibition of complex V by oligomycin allows for analysis of the contribution of ATP synthase to OXPHOS (discussed later).

Gene set enrichment analysis (GSEA) (Mootha et al., 2003; Subramanian et al., 2005) was used to assess transcript expression changes in metabolic pathways. Comparing each division after LPS stimulation to undivided cells suggested that the OXPHOS pathway was significantly upregulated in a stepwise manner (Figure 1D). Conversely, the GSEA signature for glycolysis failed to reach significant enrichment in any of the divisions.

Examples of OXPHOS genes that displayed progressive upregulation included *Sdhb*, *Atp5g2*, *Cs*, *Cox7a2*, and *Sod1* with the largest changes occurring at division 8+ (Figure 1E). *Cs* encodes citrate synthase, which catalyzes acetyl-coenzyme A (CoA) from citrate and is the first step of the TCA cycle. *Cox7a2* codes for cytochrome *c* oxidase, which is the final component of the ETC before ATP synthase and catalyzes electron transfer from cytochrome *c* to oxygen. *Sod1* encodes superoxide dismutase 1 that catalyzes the reduction of oxygen radicals in the cytoplasm (McCord and Fridovich, 1969). Thus, the transcriptome is reprogrammed to support changes in metabolic machinery between nB cells and PBs.

### T-Independent B Cell Activation Increases OXPHOS *Ex Vivo*

To determine whether gene expression and functional metabolic changes correlate, an *ex vivo* model of B cell stimulation induced by TLR4 ligation (Yoon et al., 2012) was used.

After 2 days of *ex vivo* LPS stimulation, cells had undergone up to 4 divisions, and ~15% of B cells upregulated expression of CD138 (Figure 2A). By 3 days, cells had undergone 4–6 divisions, and the number of CD138+ cells increased to 27%. At 2 days, there was a modest, statistically significant increase in OXPHOS, as measured by oxygen consumption rate (OCR), between LPS-stimulated and nB cells (Figure 2B). By 3 days, there was nearly a 10-fold increase in OCR (Figure 2B), corresponding to the increase in actB cell and PB frequency (Figure 2A). These data corroborate the gene expression data and demonstrate that use of OXPHOS is increased as B cells progress through differentiation *ex vivo*.

### PBs Rely on OXPHOS for Antibody Secretion

Given the aforementioned observation that OXPHOS increased with PB frequency, its functional requirement for antibody synthesis and secretion was determined. *Ex-vivo*-generated PBs (3 days) were treated with OXPHOS inhibitors or reactive oxygen species (ROS) manipulators, and the levels of secreted immunoglobulin M (IgM) were measured by ELISA (Figure 2C). Treatment with the ATP synthase inhibitor oligomycin (Franchi et al., 2017) resulted in a highly significant 1.5-fold decrease in antibody concentration. Other inhibitors of OXPHOS, including FCCP, antimycin A, and rotenone + antimycin A, caused similar decreases in antibody concentration (Figure 2C) without any increase in cell death (data not shown). Rotenone, a complex I inhibitor, oxidizes NADH to NAD<sup>+</sup>, which allows the ETC to progress. In the process, complex I also generates ROS (Murphy, 2009). Interestingly, neither rotenone, N-acetyl-L-cysteine (an ROS inhibitor), nor pyocyanin (an ROS inducer) impacted antibody titers (Masciarelli and Sitia, 2008). ROS were measured and found to be higher in PBs compared to actB and nB cells (Figure 2D). Likewise, superoxide species were increased upon activation but comparable between actB cells and PBs. However, because ROS inducers and inhibitors had no impact on antibody secretion, we conclude that oxidative metabolism, but not ROS, is required for maximal antibody titers.

Reduced antibody titers did not distinguish between defects in antibody production or secretion. Intracellular IgM staining and analysis by flow cytometry showed that PBs produced similar levels of IgM, regardless of oligomycin or vehicle treatment (Figure 2E). Therefore, oligomycin interferes with PB antibody secretion but not the production of IgM.

### Differentiating B Cell Subsets Increase Oxygen Consumption in a Stepwise Manner

To track the activation and differentiation state of B cells *in vivo*, two phenotypic markers were used. Activation was defined by surface expression of the sialic-acid-binding protein GL7 (Naito et al., 2007). As mentioned earlier, as B cells divide and ultimately differentiate to PBs, they acquire expression of CD138. In an *in vivo* LPS stimulation assay (Yoon et al., 2012), ~15 and 30% of the cells expressed CD138 and GL7, respectively (Figure 3A). To characterize the metabolic changes occurring at distinct phenotypic stages throughout differentiation, nB cells (GL7<sup>-</sup>CD138<sup>-</sup>), actB cells (GL7<sup>+</sup>CD138<sup>+</sup>), and PBs (CD138<sup>+</sup>) were purified by magnetic enrichment (Figure 3B), normalized to the same cell number, and their use of OXPHOS was determined. Quiescent nB cells showed minimal responses to mitochondrial stressors (Figure 3C), indicating no significant use of OXPHOS. Compared to nB cells and PBs, actB cells exhibited intermediate levels of basal respiration (Figures 3C

and 3D); and, upon uncoupling of the ETC with FCCP, their maximal OCR was also intermediate (Figure 3E). PBs displayed the highest level of OXPHOS usage; and their spare respiratory capacity (SRC), the difference between maximal and basal respiration or reserved oxidative ability, was highest among the cell types (Figure 3F). The intermediate OXPHOS levels in actB cells may indicate a transitional step in their metabolic programming.

### OXPHOS Increases PB Frequency

To test whether promoting OXPHOS would result in increased PB differentiation, nB cells were treated with dichloroacetate, stimulated with LPS, interleukin (IL)-2, and IL-5 *ex vivo* for 3 days, and the frequency of CD138+ PBs was measured by flow cytometry. Dichloroacetate inhibits pyruvate dehydrogenase kinase, promoting OXPHOS at the expense of glycolysis (Sanchez et al., 2013; Shen et al., 2013; Stockwin et al., 2010). Dichloroacetate treatment increased the total frequency of CD138+ plasmablasts and the frequency per cell division (Figure 3G). Dichloroacetate-treated cultures did not divide as extensively as vehicle-treated cultures, supporting a role for OXPHOS in differentiation of plasmablasts, but not in cell division.

### actB Cells and PBs Contain Similar Amounts of ATP

Differences in oxygen consumption between actB cells and PBs suggest that these cells may contain different amounts of ATP. Surprisingly, quantification of ATP levels in cell extracts showed that actB cells and PBs retain similar concentrations of ATP (Figure 3G). Additionally, after oligomycin treatment, ATP levels in actB cells and PBs were decreased, indicating that both cell types were sensitive to mitochondrial ATP synthase inhibition (Figure 3G). nB cells similarly showed a small but significant decrease with oligomycin treatment. Together, this suggests that rapidly proliferating actB cells use other metabolic pathways to augment their ATP production (Lunt and Vander Heiden, 2011).

### actB Cells Use Glycolysis to Supplement Their Metabolism

A glycolytic rate assay that measures glycolysis in the absence of OXPHOS was performed on the cell subsets. nB and actB cells were unresponsive to inhibition of OXPHOS, suggesting that, although these cells use OXPHOS, they were not reliant on this pathway (Figure 3H). PBs showed a compensatory increase in proton extrusion rate (PER), corroborating the results shown previously that PBs use significant OXPHOS. The specific contribution of glycolysis to PER was calculated by subtracting total PER from the CO<sub>2</sub>-derived PER produced from OXPHOS. ActB cells had a higher percentage of PER from glycolysis than both nB cells and PBs, suggesting their use of this pathway (Figure 3H).

### Blimp1-cKO B Cells Fail to Upregulate OXPHOS

As nB cells differentiate to PBs, they first become activated, proliferate, and subsequently differentiate. To determine whether metabolic changes are due to proliferation or differentiation, a *Prdm1<sup>fl/fl</sup> Cd19<sup>Cre/+</sup>* (Blimp1-cKO) mouse model was used, which does not form PBs (Shapiro-Shelef et al., 2003). To track proliferation and differentiation *in vivo*, Blimp1-cKO or wildtype (WT) B cells were labeled with CTV and adoptively transferred

into congenically marked  $\mu$ MT mice. Mice receiving WT or Blimp1-cKO splenocytes reconstituted to a similar degree (Figure 4A) and similarly expressed GL7 (Figure 4B). Cell division analysis showed that the cells divided normally (Figures 4C and 4D), suggesting that there is no *in vivo* proliferation defect caused by Blimp1 deficiency. As anticipated from the model, whereas WT B cells upregulate expression of CD138 at division 8, Blimp1-cKO cells fail to do so (Figures 4C and 4D). WT nB cells, actB cells, and PBs as well as Blimp1-cKO actB cells were magnetically enriched and tested for their use of OXPHOS. The OCR between WT and Blimp1-cKO actB cells was identical (Figure 4E) and less than that for PBs, suggesting that, despite having similar proliferation profiles, the generation of PBs and the ability for cells to reach their full metabolic capacity are concomitant. Thus, these data suggest that the Blimp1 transcriptional program is required to support the increased metabolic requirements of PBs.

## DISCUSSION

The balance between catabolism and anabolism must meet the demands of the cell type and the environment. These needs can be met by various metabolic pathways, including OXPHOS, glycolysis, and fatty acid oxidation, all of which exist in any given cell. Here, we provide evidence for a specific and ordered upregulation of the OXPHOS program during B cell differentiation in response to a T-independent antigen. This program ultimately allows PBs to utilize the OXPHOS machinery to its maximal extent, reflecting the high demand for ATP in antibody synthesis and secretion.

As B cells divide during *in vivo* differentiation to LPS, changes in metabolic programming occurred first at the level of transcription where 132 genes encoding proteins associated with both the TCA cycle and ETC were progressively increased. Succinate dehydrogenase subunits A through D were upregulated during early and late divisions, as cells progressed to PBs. In addition to converting succinate to fumarate in the TCA cycle; succinate dehydrogenase reduces ubiquinone to ubiquinol in complex II of the ETC. This enzymatic step facilitates the transfer of electrons from complex II to complex III; as such, succinate dehydrogenase aids in both the proton pump/gradient and in the transfer of electrons to the ATP synthase. In macrophages, *Sdhb* is important for expression of hypoxia inducible factor 1 alpha (HIF-1 $\alpha$ ) and IL-1 $\beta$  (Mills et al., 2016). Additionally, succinate is the downstream metabolite of the  $\alpha$ -ketoglutarate ( $\alpha$ KG) dehydrogenase complex. A high ratio of  $\alpha$ KG to succinate has been shown to promote differentiation of M2 macrophages (Liu et al., 2017). However, the role of succinate and/or succinate dehydrogenase has not been identified in circulating PBs.

Previous reports showed that 2 days after LPS stimulation *ex vivo*, Blimp1-cKO B cells had a slight proliferative advantage over WT cells (Shapiro-Shelef et al., 2003). Our *ex vivo* data showed similar results 3 days following LPS stimulation (data not shown). However, in response to LPS *in vivo*, Blimp1-cKO B cells proliferated at the same rate as WT B cells, and there were no significant differences in cell numbers at any division. The differences between *in vivo* and *ex vivo* stimulation could be attributed to cytokines or factors not present or overrepresented in an *ex vivo* culture system. Nonetheless, the Blimp1-cKO

defect observed here and previously (Shapiro-Shelef et al., 2003) was due to a block in differentiation, as measured by the failure to upregulate CD138.

PB differentiation occurs with concomitant morphological changes to support robust antibody secretion, including significant growth of the endoplasmic reticulum (ER). High levels of antibody production result in a stress response that is tempered by upregulation of the unfolded protein response (UPR) (Reimold et al., 2001). The UPR is increased upon recognition of misfolded proteins in the ER, which is usually associated with hypoxia, low glucose, or calcium imbalance. XBP-1, a transcription factor induced by the UPR in PBs (Barwick et al., 2016), is required for differentiation (Iwakoshi et al., 2003), as well as mitochondrial mass and function (Jang et al., 2015; Shaffer et al., 2004). This suggests a direct link between antibody secretion and metabolic reprogramming that we further characterized by identifying a requirement for ATP synthase in IgM secretion, as well as an increased propensity for B cells to differentiate when OXPHOS is induced by dichloroacetate.

Coupled with the transcriptional changes were observations reflecting the utilization of the OXPHOS pathway. OCR in PBs may be sensitive to redox imbalances induced by high levels of OXPHOS and protein translation. However, *Sod1* was upregulated in PBs and may temper the redox imbalances. Genes that produce the ATP synthase complex were significantly upregulated in division 8+ PBs, which was consistent with their sensitivity to oligomycin. ActB cells maintained a relatively low OCR that was similar to that of quiescent nB cells. Surprisingly, actB cells contained levels of ATP similar to those for PBs, which had a high OCR. Thus, because ATP levels were the same, an additional pathway was hypothesized to be used in actB cells. Similar to proliferating T cells, proliferating B cells upregulate glycolysis (Chang et al., 2013; MacIver et al., 2013; Michalek et al., 2011). Blimp1-cKO actB cells consumed oxygen to the same degree as WT actB cells, both of which were less than that consumed by PBs, indicating that proliferating B cells rely on glycolysis to supplement their ATP generation. ActB cells exhibited slightly higher OXPHOS than nB cells but have the potential to form PBs and are, therefore, poised to increase OXPHOS to a level similar to that of PBs at the point of differentiation. Thus, B cells are inherently programmed to increase the transcription of OXPHOS pathway genes during differentiation, and this programming is required for maximal antibody secretion.

## EXPERIMENTAL PROCEDURES

Detailed procedures for cell isolation, *ex vivo* differentiation, and the Seahorse Bioanalyzer, and antibody clones can be found in the Supplemental Experimental Procedures.

### Mice and LPS Challenge

C57/BL6J mice 8–12 weeks of age were used for experiments, with a mix of male and female mice. *Prdm1<sup>fl/fl</sup> Cd19<sup>Cre/+</sup>* (Blimp1-cKO) mice were previously generated (Shapiro-Shelef et al., 2003). *In vivo* LPS challenge was 50 µg LPS (Enzo, ALX-581-008) intravenously. Mice were analyzed 3 days after challenge. All animals were housed by the Emory Division of Animal Resources, and all protocols were approved by the Emory Institutional Animal Care and Use Committee (IACUC).

## Flow Cytometry

Cells were washed and resuspended at  $10^7$  cells per milliliter in PBs with 1% BSA and 2 mM EDTA. Cells were stained for 1 hr with antibody cocktails (see Supplemental Experimental Procedures) and fixed with 1% paraformaldehyde before analysis. Flow-cytometric analysis was collected on a Becton Dickinson (BD) LSRII, and FCS files were exported using FACSDiva (v6.2). Analysis of flow cytometry data was conducted with FlowJo software (v10).

## ATP Quantification

Cells were sorted on a BD FACSAria II and plated at 50,000 cells per well before vehicle or oligomycin treatment for 2 hr at 37 C. ATP was quantified with use of a standard curve, as per manufacturer's protocol (Abcam, #113849).

## Statistical Analysis

Statistical analyses were performed using a Student's t test. Paired analyses were used in all *in vivo* LPS-treatment experiments where actB cells and PBs were isolated from the same animal. In all other cases, a two-tailed t test was used.

## Supplementary Material

Refer to Web version on PubMed Central for supplementary material.

## Acknowledgments

We thank Dr. D. Neeld for designing and creating the graphical abstract, R. Butler for animal husbandry and care, A. Kania and R. Haines for comments and critiques of the manuscript, and K. Fife and R. Karaffa for cell sorting at the Emory Flow Cytometry Core. This work was supported by an NIH grant (1R01AI123733) to J.M.B.

## References

- Aronov M, Tirosh B. Metabolic Control of Plasma Cell Differentiation- What We Know and What We Don't Know. *J Clin Immunol*. 2016; 36(Suppl 1):12–17.
- Barwick BG, Scharer CD, Bally APR, Boss JM. Plasma cell differentiation is coupled to division-dependent DNA hypomethylation and gene regulation. *Nat Immunol*. 2016; 17:1216–1225. [PubMed: 27500631]
- Caro-Maldonado A, Wang R, Nichols AG, Kuraoka M, Milasta S, Sun LD, Gavin AL, Abel ED, Kelsoe G, Green DR, Rathmell JC. Metabolic reprogramming is required for antibody production that is suppressed in anergic but exaggerated in chronically BAFF-exposed B cells. *J Immunol*. 2014; 192:3626–3636. [PubMed: 24616478]
- Chang CH, Curtis JD, Maggi LB Jr, Faubert B, Villarino AV, O'Sullivan D, Huang SC, van der Windt GJ, Blagih J, Qiu J, et al. Post-transcriptional control of T cell effector function by aerobic glycolysis. *Cell*. 2013; 153:1239–1251. [PubMed: 23746840]
- Doughty CA, Bleiman BF, Wagner DJ, Dufort FJ, Mataraza JM, Roberts MF, Chiles TC. Antigen receptor-mediated changes in glucose metabolism in B lymphocytes: role of phosphatidylinositol 3-kinase signaling in the glycolytic control of growth. *Blood*. 2006; 107:4458–4465. [PubMed: 16449529]
- Dufort FJ, Bleiman BF, Gumina MR, Blair D, Wagner DJ, Roberts MF, Abu-Amer Y, Chiles TC. Cutting edge: IL-4-mediated protection of primary B lymphocytes from apoptosis via Stat6-dependent regulation of glycolytic metabolism. *J Immunol*. 2007; 179:4953–4957. [PubMed: 17911579]

- Fox CJ, Hammerman PS, Thompson CB. Fuel feeds function: energy metabolism and the T-cell response. *Nat Rev Immunol.* 2005; 5:844–852. [PubMed: 16239903]
- Franchi L, Monteleone I, Hao LY, Spahr MA, Zhao W, Liu X, Demock K, Kulkarni A, Lesch CA, Sanchez B, et al. Inhibiting Oxidative Phosphorylation In Vivo Restrains Th17 Effector Responses and Ameliorates Murine Colitis. *J Immunol.* 2017; 198:2735–2746. [PubMed: 28242647]
- Guzy RD, Sharma B, Bell E, Chandel NS, Schumacker PT. Loss of the SdhB, but not the SdhA, subunit of complex II triggers reactive oxygen species-dependent hypoxia-inducible factor activation and tumorigenesis. *Mol Cell Biol.* 2008; 28:718–731. [PubMed: 17967865]
- Iwakoshi NN, Lee AH, Vallabhajosyula P, Otipoby KL, Rajewsky K, Glimcher LH. Plasma cell differentiation and the unfolded protein response intersect at the transcription factor XBP-1. *Nat Immunol.* 2003; 4:321–329. [PubMed: 12612580]
- Jang KJ, Mano H, Aoki K, Hayashi T, Muto A, Nambu Y, Takahashi K, Itoh K, Taketani S, Nutt SL, et al. Mitochondrial function provides instructive signals for activation-induced B-cell fates. *Nat Commun.* 2015; 6:6750. [PubMed: 25857523]
- Lam WY, Becker AM, Kennerly KM, Wong R, Curtis JD, Llufrío EM, McCommis KS, Fahrman J, Pizzato HA, Nunley RM, et al. Mitochondrial Pyruvate Import Promotes Long-Term Survival of Antibody-Secreting Plasma Cells. *Immunity.* 2016; 45:60–73. [PubMed: 27396958]
- Liu PS, Wang H, Li X, Chao T, Teav T, Christen S, Di Conza G, Cheng WC, Chou CH, Vavakova M, et al.  $\alpha$ -ketoglutarate orchestrates macrophage activation through metabolic and epigenetic reprogramming. *Nat Immunol.* 2017; 18:985–994. [PubMed: 28714978]
- Lunt SY, Vander Heiden MG. Aerobic glycolysis: meeting the metabolic requirements of cell proliferation. *Annu Rev Cell Dev Biol.* 2011; 27:441–464. [PubMed: 21985671]
- MacIver NJ, Michalek RD, Rathmell JC. Metabolic regulation of T lymphocytes. *Annu Rev Immunol.* 2013; 31:259–283. [PubMed: 23298210]
- Masciarelli S, Sitia R. Building and operating an antibody factory: redox control during B to plasma cell terminal differentiation. *Biochim Biophys Acta.* 2008; 1783:578–588. [PubMed: 18241675]
- McCord JM, Fridovich I. Superoxide dismutase. An enzymic function for erythrocuprein (hemocuprein). *J Biol Chem.* 1969; 244:6049–6055. [PubMed: 5389100]
- Michalek RD, Gerriets VA, Jacobs SR, Macintyre AN, MacIver NJ, Mason EF, Sullivan SA, Nichols AG, Rathmell JC. Cutting edge: distinct glycolytic and lipid oxidative metabolic programs are essential for effector and regulatory CD4<sup>+</sup> T cell subsets. *J Immunol.* 2011; 186:3299–3303. [PubMed: 21317389]
- Mills EL, Kelly B, Logan A, Costa AS, Varma M, Bryant CE, Touloumou P, Dabritz JH, Gottlieb E, Latorre I, et al. Succinate Dehydrogenase Supports Metabolic Repurposing of Mitochondria to Drive Inflammatory Macrophages. *Cell.* 2016; 167:457–470.e13. [PubMed: 27667687]
- Mootha VK, Lindgren CM, Eriksson KF, Subramanian A, Sihag S, Lehar J, Puigserver P, Carlsson E, Ridderstråle M, Laurila E, et al. PGC-1 $\alpha$ -responsive genes involved in oxidative phosphorylation are coordinately downregulated in human diabetes. *Nat Genet.* 2003; 34:267–273. [PubMed: 12808457]
- Murphy MP. How mitochondria produce reactive oxygen species. *Biochem J.* 2009; 417:1–13. [PubMed: 19061483]
- Naito Y, Takematsu H, Koyama S, Miyake S, Yamamoto H, Fujinawa R, Sugai M, Okuno Y, Tsujimoto G, Yamaji T, et al. Germinal center marker GL7 probes activation-dependent repression of N-glycolylneuraminic acid, a sialic acid species involved in the negative modulation of B-cell activation. *Mol Cell Biol.* 2007; 27:3008–3022. [PubMed: 17296732]
- Reimold AM, Iwakoshi NN, Manis J, Vallabhajosyula P, Szomolanyi-Tsuda E, Gravallesse EM, Friend D, Grusby MJ, Alt F, Glimcher LH. Plasma cell differentiation requires the transcription factor XBP-1. *Nature.* 2001; 412:300–307. [PubMed: 11460154]
- Sanchez WY, McGee SL, Connor T, Mottram B, Wilkinson A, White-head JP, Vuckovic S, Catley L. Dichloroacetate inhibits aerobic glycolysis in multiple myeloma cells and increases sensitivity to bortezomib. *Br J Cancer.* 2013; 108:1624–1633. [PubMed: 23531700]
- Shaffer AL, Shapiro-Shelef M, Iwakoshi NN, Lee AH, Qian SB, Zhao H, Yu X, Yang L, Tan BK, Rosenwald A, et al. XBP1, downstream of Blimp-1, expands the secretory apparatus and other

- organelles, and increases protein synthesis in plasma cell differentiation. *Immunity*. 2004; 21:81–93. [PubMed: 15345222]
- Shapiro-Shelef M, Lin KI, McHeyzer-Williams LJ, Liao J, McHeyzer-Williams MG, Calame K. Blimp-1 is required for the formation of immunoglobulin secreting plasma cells and pre-plasma memory B cells. *Immunity*. 2003; 19:607–620. [PubMed: 14563324]
- Shen YC, Ou DL, Hsu C, Lin KL, Chang CY, Lin CY, Liu SH, Cheng AL. Activating oxidative phosphorylation by a pyruvate dehydrogenase kinase inhibitor overcomes sorafenib resistance of hepatocellular carcinoma. *Br J Cancer*. 2013; 108:72–81. [PubMed: 23257894]
- Smith KG, Hewitson TD, Nossal GJ, Tarlinton DM. The phenotype and fate of the antibody-forming cells of the splenic foci. *Eur J Immunol*. 1996; 26:444–448. [PubMed: 8617316]
- Stockwin LH, Yu SX, Borgel S, Hancock C, Wolfe TL, Phillips LR, Hollingshead MG, Newton DL. Sodium dichloroacetate selectively targets cells with defects in the mitochondrial ETC. *Int J Cancer*. 2010; 127:2510–2519. [PubMed: 20533281]
- Subramanian A, Tamayo P, Mootha VK, Mukherjee S, Ebert BL, Gillette MA, Paulovich A, Pomeroy SL, Golub TR, Lander ES, Mesirov JP. Gene set enrichment analysis: a knowledge-based approach for interpreting genome-wide expression profiles. *Proc Natl Acad Sci USA*. 2005; 102:15545–15550. [PubMed: 16199517]
- Woodland RT, Fox CJ, Schmidt MR, Hammerman PS, Opferman JT, Korsmeyer SJ, Hilbert DM, Thompson CB. Multiple signaling pathways promote B lymphocyte stimulator dependent B-cell growth and survival. *Blood*. 2008; 111:750–760. [PubMed: 17942753]
- Yoon HS, Scharer CD, Majumder P, Davis CW, Butler R, Zinzow-Kramer W, Skountzou I, Koutsonanos DG, Ahmed R, Boss JM. ZBTB32 is an early repressor of the CIITA and MHC class II gene expression during B cell differentiation to plasma cells. *J Immunol*. 2012; 189:2393–2403. [PubMed: 22851713]

**Highlights**

- Activated B cells are poised to increase oxidative phosphorylation
- Plasmablasts require oxidative metabolism to sustain antibody secretion
- Proliferation alone is unable to fully induce oxidative phosphorylation in B cells
- Expression of Blimp1 is required for maximal metabolic activity

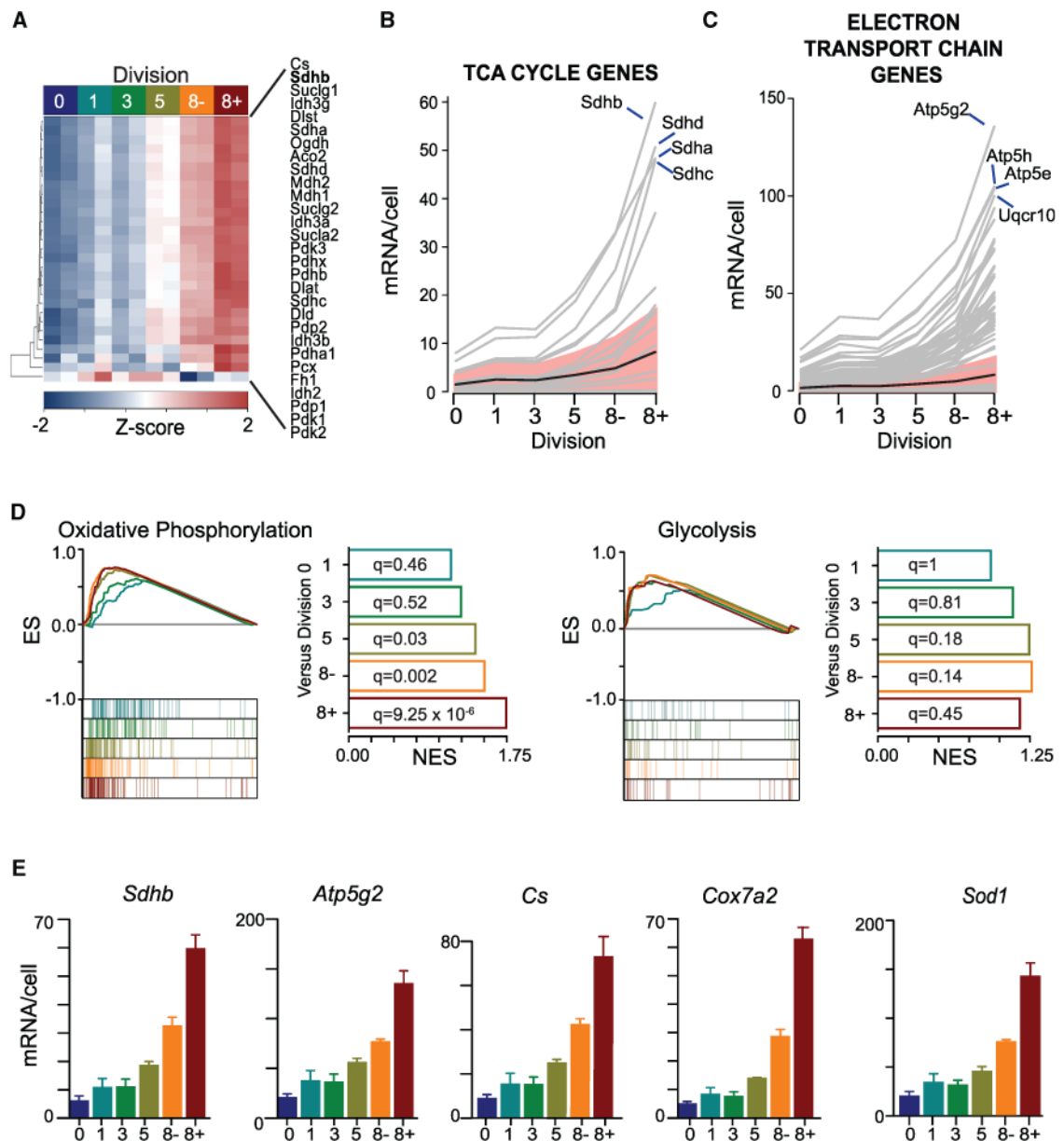


**Figure 1. PBs Specifically Upregulate Genes Involved in OXPHOS**

(A) Heatmap analysis of tricarboxylic acid (TCA) cycle gene expression data from Barwick et al. (2016), in which B cells undergoing *in vivo* proliferation were isolated by cell division and CD138 expression. Expression is indicated by *Z* score.

(B) mRNA expression plots of TCA cycle genes across cell divisions from (A). The bold line indicates average gene change by division across the genome, with SD shaded in pink.

(C) mRNA expression plots of electron transport chain (ETC) genes in each division are indicated as in (B).

(D) GSEA for “Reactome\_TCA cycle and respiratory electron transport” (Oxidative Phosphorylation) and “Reactome\_Glycolysis” (Glycolysis) are shown and quantified by normalized enrichment score (NES). *q* values for the comparison between division 0 and the other divisions are shown.

(E) Example gene expression bar graphs per cell division are shown from RNA-sequencing data described in (A). Data are plotted as mean  $\pm$  SD.

Author Manuscript

Author Manuscript

Author Manuscript

Author Manuscript

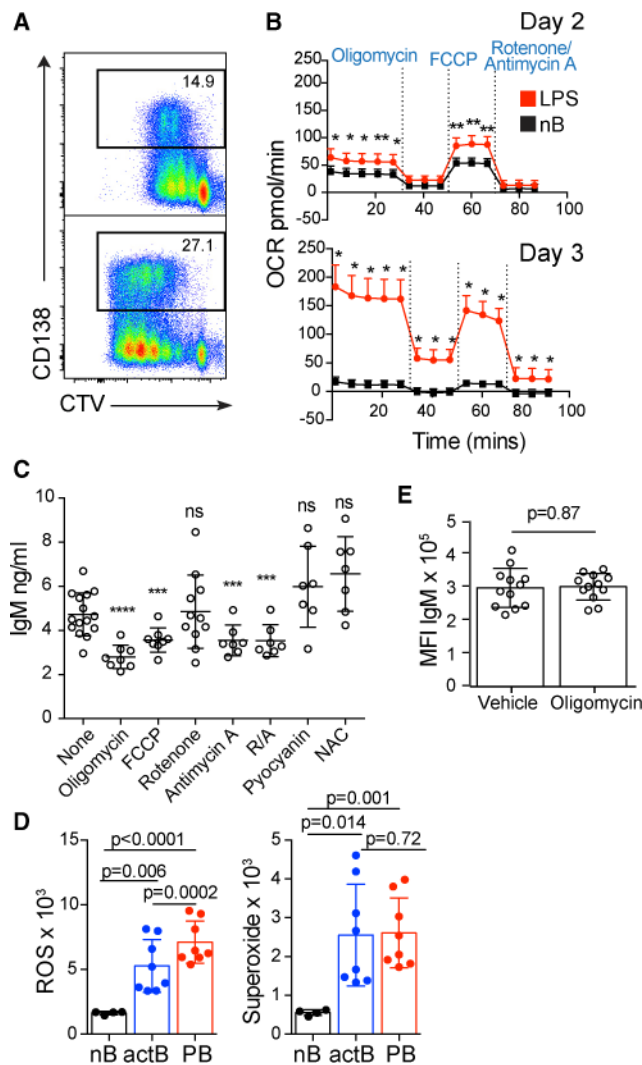


### Figure 2. LPS Stimulation Induces B Cell Differentiation and Increases OXPHOS

(A) B cells were labeled with CTV and cultured for 2 (top) and 3 (bottom) days, as indicated, in the presence of LPS, IL-2, and IL-5. CTV dilution and CD138 expression were analyzed by flow cytometry. The percentage of total CD138<sup>+</sup> cells is highlighted.

(B) Cells from (A) were analyzed by mitochondrial stress test on a Seahorse XFe96 Bioanalyzer, and the results were plotted. The addition of metabolic inhibitors is indicated. Data for (A) and (B) were generated from two independent groups of 2 control mice and 4 LPS-treated mice each. Data are plotted as mean  $\pm$  SD. \* $p < 0.001$ , \*\* $p < 0.01$ .

(C) nB cells were stimulated for 3 days, washed, and plated in fresh media with the indicated drug for 2 hr, and then the supernatant was assayed for IgM secretion by ELISA. Data are indicated as mean  $\pm$  SD and were derived from three independent groups of 3–5 mice. ns, not significant. \*\*\* $p < 0.001$  and \*\*\*\* $p < 0.0001$ .

(D) Reactive oxygen species and superoxide levels were measured by flow cytometry. Data are indicated mean  $\pm$  SD and are representative of two groups of 4 mice each.

(E) The cells from cultures in (C) treated with vehicle control or oligomycin were permeabilized and stained for intracellular IgM and assessed by flow cytometry. Data are indicated as mean  $\pm$  SD and were derived from three independent groups of 4 mice each.

Author Manuscript

Author Manuscript

Author Manuscript

Author Manuscript

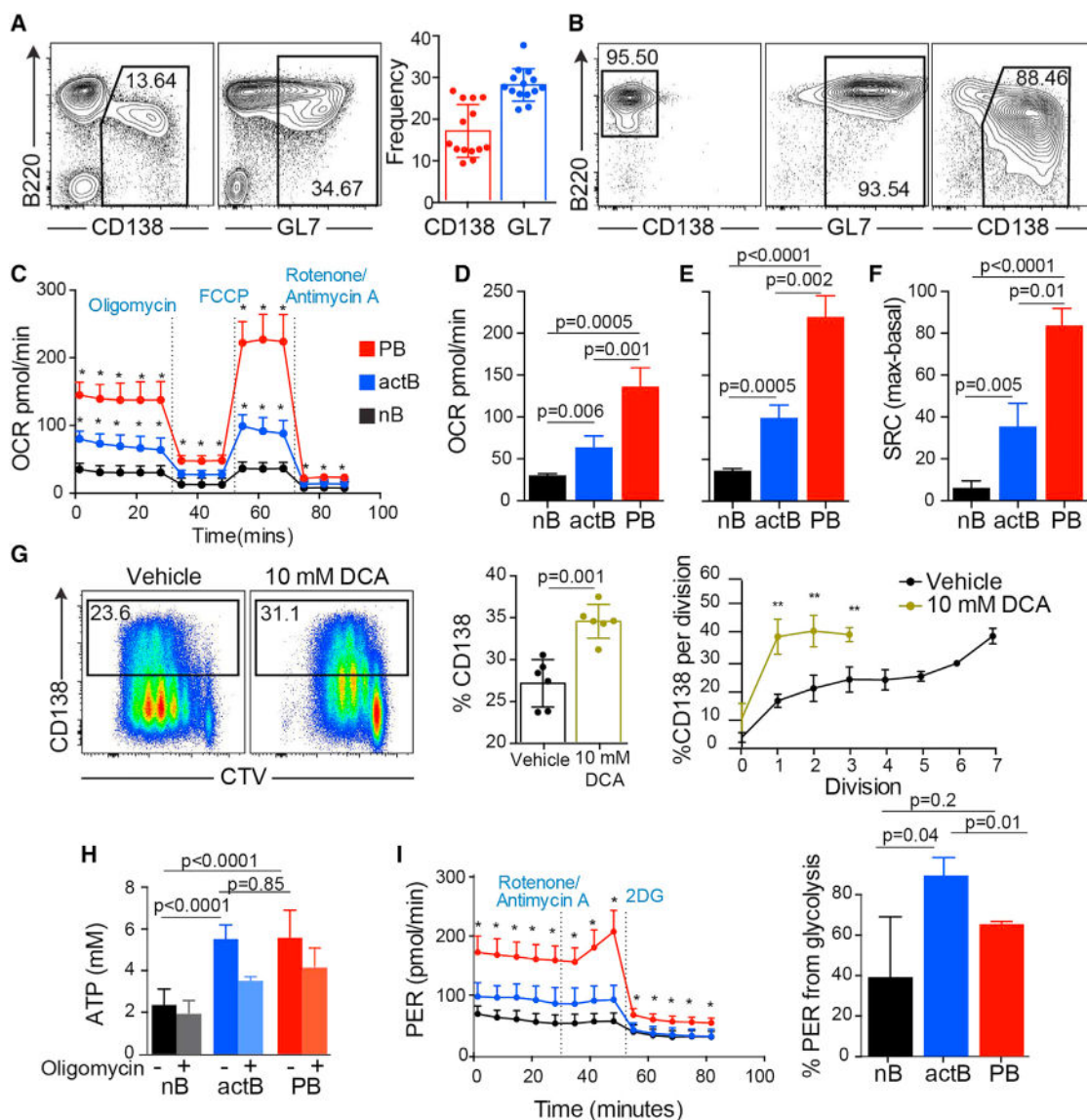


### Figure 3. B Cells Progressively Upregulate OXPHOS after LPS Stimulation *In Vivo*

(A) Flow cytometry plot for nB cells (B220), actB cells (GL7), and PBs (CD138) from spleens of mice inoculated with LPS intravenously (i.v.) (left). Summary data of cell frequencies (right). Data are indicated as mean  $\pm$  SD and represent three groups of 3 mice each.

(B) Representative flow cytometry plots of nB cells from PBS-treated mice and actB cells and PBs from LPS-treated mice following magnetic enrichment. Purity frequencies are indicated. Data are representative of 3 groups each containing 3 control and 4–5 LPS-treated mice.

(C) Enriched subsets from (B) were analyzed by mitochondrial stress test as in Figure 2B. Data represent mean  $\pm$  SD of one group of three; each group contained 3 control and 4–5 LPS-treated mice. \*  $p < 0.0001$ .

(D) Summary data from (C) showing basal OCR (final time point prior to oligomycin), mean  $\pm$  SD.

(E) Summary data from (C) showing maximal OCR (first time point following FCCP), mean  $\pm$  SD.

(F) Summary data from (C) showing spare respiratory capacity (maximal basal), mean  $\pm$  SD.

(G) Representative flow cytometry plots of naive B cells cultured with vehicle or 10 mM dichloroacetate (DCA). Total frequency of CD138<sup>+</sup> PBs and frequency per division are plotted at the right. Data are representative of mean  $\pm$  SD of two experiments with 3 mice each.

(H) ATP concentration was determined from FACS-isolated cell populations, as described in the Experimental Procedures, with or without oligomycin. Purity of these populations was >95% (data not shown). Data represent mean  $\pm$  SD of 2 groups each of 2 control and 5 LPS-treated mice.

(I) GL7<sup>+</sup> and CD138<sup>+</sup> positively selected B cells were analyzed by glycolytic rate assay. % PER from glycolysis was calculated as (basal glycolysis)/(basal PER)  $\times$  100%. Data are indicated as mean  $\pm$  SD and represent one group of two, each containing 3 control and 5 LPS-treated mice. \*p < 0.01.

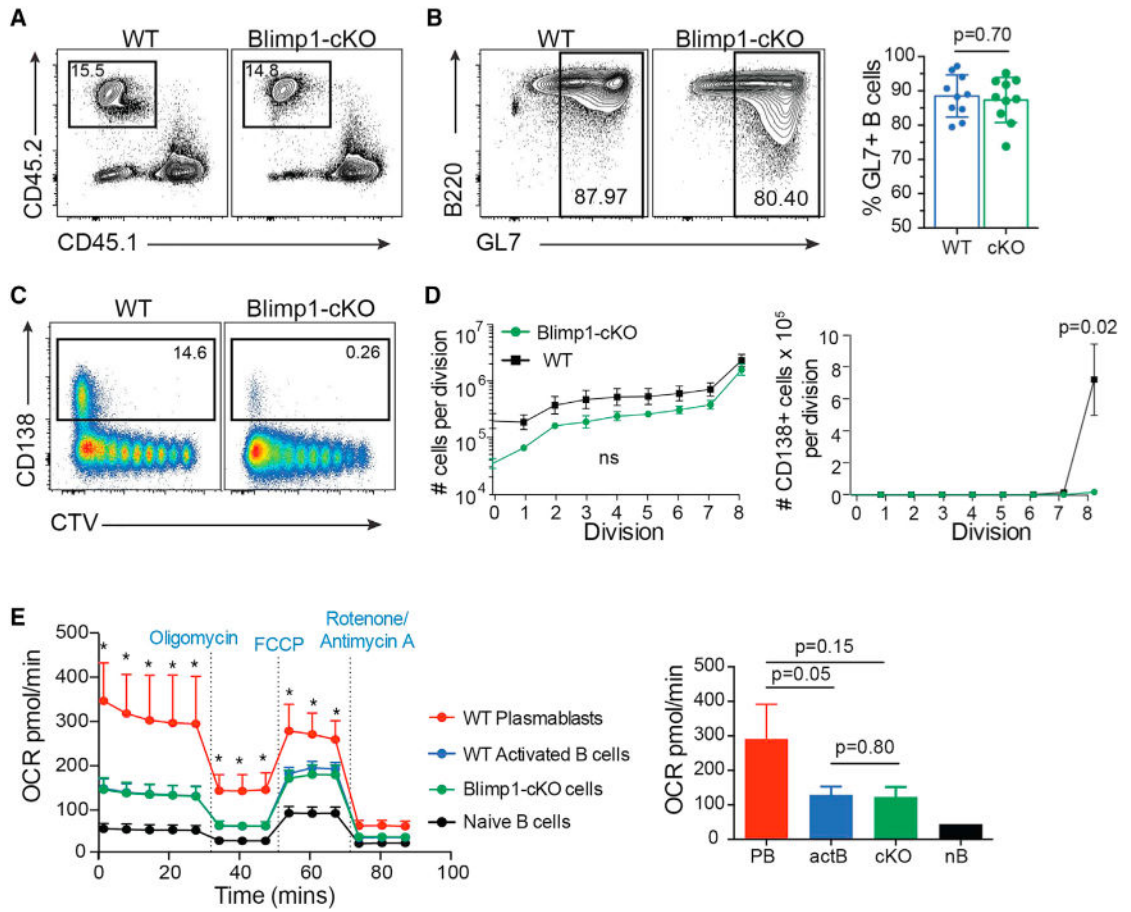


**Figure 4. Blimp1 cKO B cells Fail to Upregulate OXPHOS**

(A) CD45.2+ Blimp1-cKO or WT littermate B cells were labeled with CTV and adoptively transferred into CD45.1+  $\mu$ MT mice. 24 hr later, mice were inoculated with LPS and analyzed at 3 days by flow cytometry. Reconstitution of WT and Blimp1-cKO B cells is shown.

(B) Transferred WT and Blimp1-cKO B cells were analyzed for expression of activation marker GL7. Representative flow plots and averaged frequencies (mean  $\pm$  SD) are shown.

(C) Representative flow cytometry displaying cell division (CTV) and PB (CD138) status of WT or Blimp1-cKO B cells after adoptive transfer.

(D) Summary plots (mean  $\pm$  SD) from (C) of total cell numbers in each division after LPS challenge (left) and CD138+ cells in each division after LPS challenge (right). Data are derived from three groups of 3–5 WT and cKO mice each. ns, not significant.

(E) nB cells, positively selected GL7+ actB WT and Blimp1-cKO cells, and CD138+ PBs were analyzed by mitochondrial stress test (left) as in Figure 2B. GL7+ and CD138+ cells were magnetically enriched to 90 and 80% purity, respectively. Basal OCR of samples was measured at the last time point prior to oligomycin (right). Data are representative of one of three independent experiments containing 3–5 WT and Blimp1-cKO mice each. \*p < 0.001; ns, not significant.

Author Manuscript

Author Manuscript

Author Manuscript

Author Manuscript